Journal of Photochemistry and Photobiology A: Chemistry 270 (2013) 75–84

Contents lists available at ScienceDirect

Journal of Photochemistry and Photobiology A: Chemistry

journal homepage: www.elsevier.com/locate/jphotochem

Spectroscopic and photodynamic properties of 5,10,15,20-tetrakis[4-(3-*N*,*N*-dimethylaminopropoxy)phenyl]porphyrin and its tetracationic derivative in different media

S. Jimena Mora, M. Elisa Milanesio, Edgardo N. Durantini *

Departamento de Química, Facultad de Ciencias Exactas Físico-Químicas y Naturales, Universidad Nacional de Río Cuarto, Agencia Postal Nro 3, X5804BYA Río Cuarto, Córdoba, Argentina

ARTICLE INFO

Article history:
Received 1 May 2013
Received in revised form 21 July 2013
Accepted 25 July 2013
Available online xxx

Keywords:
Porphyrin
Photosensitizer
Singlet oxygen
Micelles
Cyclodextrin

ABSTRACT

The spectroscopic properties and the photodynamic activity of 5,10,15,20-tetrakis[4-(3-*N*,*N*-dimethylaminopropoxy)phenyl]porphyrin (TAPP) and its tetracationic derivative ($TAPP^{4+}$) were studied in homogeneous media and in microheterogeneous systems. The results were compared with those of 5,10,15,20-tetra(4-*N*,*N*,*N*-trimethylammoniumphenyl)porphyrin ($TMAP^{4+}$), which represents an active tetracationic photosensitizer. Absorption and fluorescence studies indicated that the tetrapyrrolic macrocycle retains its individual spectroscopic properties. Interaction with β-cyclodextrin (β-CD) was found for $TAPP^{4+}$ by fluorescence emission. Also, these porphyrins interact with *n*-heptane/sodium bis(2-ethylhexyl)sulfosuccinate (AOT)/water reverse micelles. Photosensitization ability was evaluated using 9,10-dimethylanthracene in *N*,*N*-dimethylformamide and AOT micelles, while tetrasodium 2,2′-(anthracene-9,10-diyl)bis(methylmalonate) was used in aqueous solutions. Also, photosensitized decomposition of L-tryptophan was investigated in these media. In particular, Trp was fast photooxidized by TAPP in a biomimetic media formed by AOT reverse micelles. Therefore, this intrinsically non-charged porphyrin represents an interesting photosensitizer for the photodynamic inactivation of microorganisms.

1. Introduction

Porphyrins containing cationic substituents have attracted considerable interest because of their notable ability as photother-apeutic agents. In particular, positively charged porphyrins have been proposed for the eradication of microbial infections by photodynamic inactivation (PDI) [1]. Basically, PDI is based on the administration of a photosensitizer, which is preferentially accumulated in microbial cells. Upon aerobic irradiation with visible light, highly reactive oxygen species (ROS) are generated in the cells. These ROS rapidly react with a variety of biomolecules producing a loss of biological functionality that lead to cellular inactivation [2]. Therefore, adequate photosensitizers are deemed to have specific chemical and biological properties. Two of the photochemical requisites are a high absorption coefficient in the visible region of the spectrum and a long lifetime of triplet excited state to produce efficiently ROS. In general, two photoprocesses can be mainly involved after activation of the photosensitizer [3]. In the type I pathway, the photosensitizer interacts with substrates to produce free radicals. These radicals can react with oxygen yielding a complex mixture of ROS. While in the type II mechanism, singlet molecular oxygen, $O_2(^1\Delta_g)$, is produced by energy transfer from the photosensitizer. Thus, the prevailing mechanism can be influenced by the photosensitizer, the presence of substrates and the microenvironment where the agent is located.

Several porphyrins with intrinsic positive charges have been successfully tested as photoinactivating agents against microorganisms [1,2]. In particular, the positive charges on the tetrapyrrolic macrocycle appear to promote a tight electrostatic interaction with negatively charged sites at the outer surface of the Gram-negative bacteria, increasing the efficiency of the photoinactivation processes [1]. Moreover, the studies have shown that non-cationic porphyrin conjugated with polylysine oligomer can efficiently promote the photoinactivation of Gram-negative bacteria [4]. In these compounds, the cationic charges are present because they are covalently bound to polylysine oligomer, which is positively charged at physiological pH values.

In previous work, the photodynamic activity of cationic porphyrin derivatives bearing 4-(3-*N*,*N*,*N*-trimethylammoniumpropoxy)phenyl substituents were investigated to inactivate *Escherichia coli* cells [5,6]. The photocytotoxic effect induced by 5,10,15,20-tetrakis[4-(3-*N*,*N*,

* Corresponding author. Tel.: +54 358 4676157; fax: +54 358 4676233.
E-mail address: edurantini@exa.unrc.edu.ar (E.N. Durantini).

1010-6030/$ – see front matter © 2013 Elsevier B.V. All rights reserved.
http://dx.doi.org/10.1016/j.jphotochem.2013.07.013

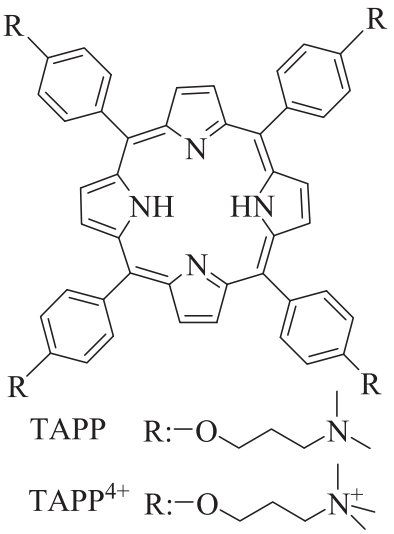

Scheme 1. Molecular structures of the studied porphyrins.

N-trimethylammoniumpropoxy)phenyl] porphyrin iodide ($TAPP^{4+}$) was quite similar to that produced by 5,10,15,20-tetrakis(4-*N*,*N*,*N*-trimethylammoniumphenyl)porphyrin ($TMAP^{4+}$), which is a standard active sensitizer established to eradicate *E. coli* and the yeast *Candida albicans* [7,8].

In the present work, the spectroscopic and photodynamic properties of 5,10,15,20-tetrakis[4-(3-*N*,*N*-dimethylammoniumpropoxy)phenyl]porphyrin (TAPP) were compared with those of $TAPP^{4+}$ and $TMAP^{4+}$ in homogeneous and microheterogeneous media (Scheme 1). The mainly deference between these porphyrins is the presence of intrinsic cationic charges in $TAPP^{4+}$ and $TMAP^{4+}$ in contrast with TAPP, which is substituted by four aliphatic amine groups. These basis amine groups in the periphery of TAPP could acquire positive charges favoring a better interaction with biomembranes, depending on the medium in which the porphyrin is located [7]. Therefore, these studies provide insights into the photodynamic activity of cationic and non-charged porphyrins in different media especially in a simple biomimetic media formed by reverse micelles and in β-cyclodextrin.

2. Materials and methods

2.1. General

All the chemicals from Aldrich (Milwaukee, WI, USA) were used without further purification. Sodium bis(2-ethylhexyl)sulfosuccinate (AOT) from Sigma (St. Louis, MO, USA) was dried under vacuum. β-Ciclodextrin (β-CD) was purchased from Aldrich. Solvents (GR grade) from Merck (Darmstadt, Germany) were distilled. Ultrapure water was obtained from a Labconco (Kansas, MO, USA) equipment model 90901-01.

2.2. Porphyrins

5,10,15,20-Tetrakis(4-*N*,*N*,*N*-trimethylammoniumphenyl) porphyrin *p*-tosylate ($TMAP^{4+}$), 5,10,15,20-tetrakis(4-sulphonatophenyl)porphyrin sodium salt ($TPPS^{4-}$) and 5,10,15,20-tetrakis(phenyl)porphyrin (TPP) were purchased from Aldrich. 5,10,15,20-tetrakis[4-(3-*N*,*N*-dimethylammoniumpropoxy)phenyl] porphyrin (TAPP) was synthesized as previously described and methylated with dimethyl sulfate to obtain 5,10,15,20-tetrakis[4-(3-*N*,*N*,*N*-trimethylammoniumpropoxy)phenyl]porphyrin ($TAPP^{4+}$) [6].

2.3. Preparation of tetrasodium 2,2′-(anthracene-9,10-diyl)bis(methylmalonate) (ABMM)

The fluorescent ABMM probe was prepared by treating 2,2′-(anthracene-9,10-diyl)bis(methylmalonic acid) (ABMA, 22 mg, 0.054 mmol), suspended in water (1.5 mL), with NaOH (11 mg, 0.27 mmol), followed by ultrasonication for a period of 5 min to give a clear solution. The tetrasodium salt product was precipitated upon the addition of ethanol. The solids were washed three times with ethanol and dried in vacuum to yield ABMM in 80% (21 mg) [9].

2.4. Spectroscopic studies

Absorption and fluorescence spectra were recorded on a Shimadzu UV-2401PC spectrometer (Shimadzu Corporation, Tokyo, Japan) and on a Spex FluoroMax spectrofluorometer (Horiba Jobin Yvon Inc, Edison, NJ, USA), respectively. The measurements were performed at 25.0 ± 0.5 °C using 1 cm path length quartz cells. The fluorescence quantum yield (Φ_F) of porphyrins were calculated by comparison of the area below the corrected emission spectrum in *N*,*N*-dimethylformamide (DMF) with that of $TMAP^{4+}$ as a reference ($\Phi_F = 0.12$) [10]. Absorbances of sample and reference were matched at the excitation wavelength ($\lambda_{exc} = 515$ nm) and the areas of the emission spectra were integrated in the range 600–800 nm. The energy of the singlet-state (E_s) was deduced from the intersection of the normalized absorption and fluorescence curves. Singlet excited state deactivation of porphyrin by L-tryptophan (Trp) was investigated using: Stern-Volmer's Eq. (1) [11]:

$$\frac{I_0}{I} = 1 + k_q \tau_0 [Q] = 1 + K_{SV}[Q] \quad (1)$$

where I_0 and I are the fluorescence intensity of porphyrin in the absence and in the presence of quencher, k_q represents the biomolecule quenching rate constant, τ_0 the excited state lifetime of in the absence of Trp, [Q] is the Trp concentration and K_{SV} is the Stern-Volmer quenching constants.

2.5. Studies in aqueous β-CD solutions

A stock solution of β-CD (0.025 M) was prepared by dissolving appropriate amount of solid material in water by stirring at 40 °C. Aliquot of this solution was transferred into 2 mL of a solution of porphyrin in water (0.2 μM) using a calibrated microsyringe. The mixed solution was thoroughly shaken. After allowed to equilibrate for 5 min, the fluorescence emission spectra were taken with an excitation wavelength at Soret band. The equilibrium binding constants ($K_{\beta\text{-CD}}$) were determined by measuring the fluorescence intensities of porphyrin at wavelength of maximum emission as a function of different β-CD concentrations. Because a large excess of β-CD relative to porphyrin was employed, it was assumed that [β-CD] ≫ [porphyrin] and therefore the data were analyzed by curve fitting method using Eq. (2) [12]:

$$I = \frac{I_0 + I_\infty K_{\beta\text{-CD}}[\beta\text{-CD}]_0^n}{1 + K_{\beta\text{-CD}}[\beta\text{-CD}]_0^n} \quad (2)$$

where I_0 and I denote the fluorescence intensity of porphyrin in the absence and in the presence of excess of β-CD, respectively; $[\beta\text{-CD}]_0$ is the analytical concentration of β-CD and n is the stoichiometric coefficient of β-CD in the formation of inclusion complexes.

2.6. Studies in AOT reverse micelles

Measurements in reverse micelles were performed using a stock solution of 0.1 M AOT, which was prepared by weighing and

dilution in *n*-heptane. The addition of water to the corresponding solution was performed using a calibrated microsyringe. The amount of water present in the system was expressed as the molar ratio between water and the AOT present in the reverse micelle ($W_0 = [H_2O]/[AOT]$). In all experiments, $W_0 = 10$ was used. The mixtures were sonicated for about 10 s to obtain perfectly clear micellar system [13].

The distribution of porphyrin between the AOT reverse micelles and the external solvent was treated considering the two pseudophase model [14]. The distribution constant, $K_{AOT} = [\text{porphyrin}_b]/[\text{porphyrin}_f][AOT]$ (where [AOT] is the surfactant concentration and the terms $[\text{porphyrin}_b]$ and $[\text{porphyrin}_f]$ refer to the concentration of bound and free porphyrin, respectively) were determined from the spectral changes at the Soret band upon varying the AOT concentration. Values of K_{AOT} were calculated by nonlinear fitting of the experimental data using Eq. (3):

$$A^{\lambda} = \frac{[\text{porphyrin}]_0(\varepsilon_f + \varepsilon_b K_{AOT}[AOT])}{(1 + K_{AOT}[AOT])} \quad (3)$$

where A^{λ} is the absorbance at different [AOT], $[\text{porphyrin}]_0$ is the initial concentration of the porphyrin, ε_f and ε_b are the molar extinction coefficients for the porphyrin in the *n*-heptane and bound to the interface, respectively. This equation applies at a fixed value of W_0 and when $[\text{porphyrin}]_0 \ll [AOT]$.

2.7. Steady state photolysis

Solutions of 9,10-dimethylanthracene (DMA, 35 μM) in organic solvents or ABMM (35 μM) in water were irradiated in 1 cm path length quartz cells (2 mL) containing the porphyrin (absorbance at Soret band ~0.3) in the different media. The samples were irradiated with monochromatic light at the porphyrin Soret band from a Novamat 130 AF slide projector (Braun Photo Technik, Nürnberg, Germany) equipped with a 150 W lamp through a high intensity grating monochromator (Photon Technology Instrument, Birmingham, NJ, USA). The light fluence rate was determined as 0.30 mW/cm^2 (Radiometer Laser Mate-Q, Coherent, Santa Clara, CA, USA). The kinetics of DMA and ABMM photooxidation were studied by following the decrease of the absorbance at $\lambda_{max} = 378$ nm. The studies in the presence of Trp (25 μM) were performed irradiating the samples with visible light (90 mW/cm^2). The light was filtered through a 2.5 cm glass cuvette filled with water to absorb heat. A wavelength range between 350 and 800 nm was selected by optical filters [15]. The kinetics of Trp decomposition were studied by following the decrease of the fluorescence intensity at $\lambda = 350$ nm. The Trp fluorescence was excited by 290 nm light. The observed rate constants (k_{obs}) were obtained by a linear least-squares fit of the semilogarithmic plot of ln A_0/A *vs.* time for DMA and ABMM, and ln I_0/I *vs.* time for Trp. All the experiment were performed at 25.0 ± 0.5 °C. The pooled standard deviation of the kinetic data, using different prepared samples, was less than 10%. Photooxidation of DMA was also used to determine $O_2(^1\Delta_g)$ production by the photosensitizers using $TMAP^{4+}$ ($\Phi_\Delta = 0.65$ in DMF) and TPP ($\Phi_\Delta = 0.62$ in toluene and tetrahydrofuran, THF) as references [5,16]. Measurements of the sample and reference under the same conditions afforded the Φ_Δ for the porphyrin by direct comparison of the slopes in the linear region of the plots [17].

3. Results and discussion

3.1. Absorption and fluorescence spectroscopic properties

The absorption spectra of porphyrins in DMF are shown in Fig. 1. These photosensitizers showed the typical Soret band at ~422 nm and the four Q-bands between 515 and 650 nm, characteristic of *meso*-tetraphenylporphyrin derivatives [18]. The Q band

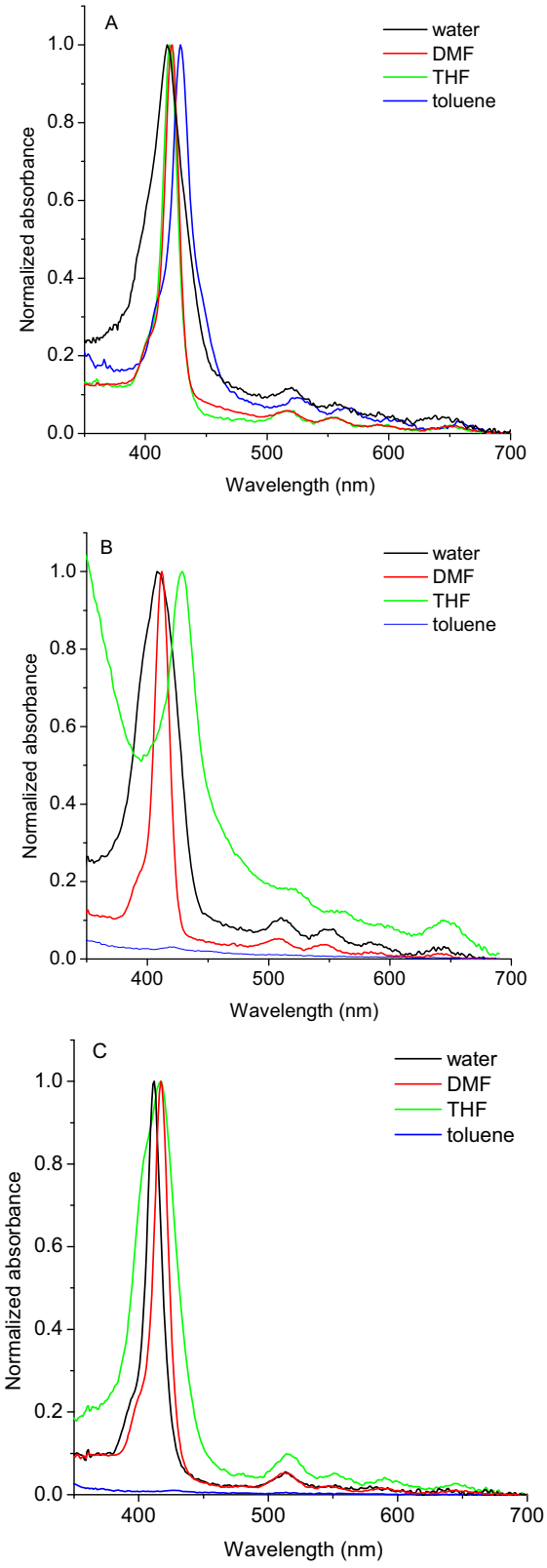

Fig. 1. Absorption spectra (A) TAPP, (B) $TAPP^{4+}$ and (C) $TMAP^{4+}$ in different solvents.

of the free base porphyrin consists of four components: $Q_x(0,0)$, $Q_x(1,0)$, $Q_y(0,0)$ and $Q_y(1,0)$, which are associated with D_{2h} symmetry [19,20]. The maximum of Soret band of TAPP and $TAPP^{4+}$ present a ~5 nm batochromic shift respect to $TMAP^{4+}$ due to the auxochromic effect of the four ether groups. Sharp absorption bands

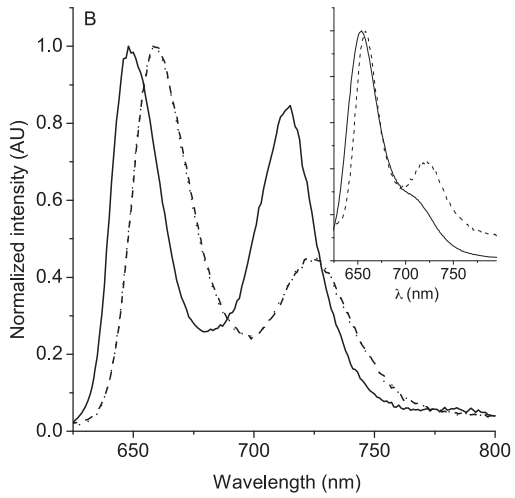

Fig. 2. Fluorescence emission spectra in DMF of TAPP (dashed line), $TAPP^{4+}$ (dotted line) and $TMAP^{4+}$ (solid line). Inset: fluorescence emission spectra in water, λ_{exc} = 515 nm.

were obtained in every case indicating that these porphyrins are mainly dissolved as monomer in DMF.

The spectra were also compared in solvents of different polarities (Fig. 1). In water, the shape of absorption bands is quite similar between TAPP and $TAPP^{4+}$. A small hypsochromic effect of 4 nm in the maximum of Soret band was produced in water with respect to DMF. Moreover, it can be observed a small broadening of these bands with respect to that of $TMAP^{4+}$ possibly due to some partial aggregation. The spectrum of TAPP in THF was very similar to that in DMF, indicting no aggregation. However, in this solvent a broadening of the Soret band was mainly observed for $TAPP^{4+}$ and in a smaller extent for $TMAP^{4+}$. In toluene, the Soret band of TAPP was bathochromically shifted by 6 nm with respect to DMF, while the charged porphyrins, $TAPP^{4+}$ and $TMAP^{4+}$, were practically insoluble in this solvent. The results in Fig. 1 indicate that absorption of the Soret band is red-shifted with a decrease in the solvent polarity. Similar behavior was previously found for water-soluble cationic porphyrins, such as 5,10,15,20-tetrakis(4-*N*-methylpyridiniumyl)porphyrin and 5-[4-(5-carboxy-1-butoxy)-phenyl]-10,15,20-tris(4-*N*-methylpyridiniumyl)porphyrin, in different solvents [21,22]. Also, it was observed that the Soret band of 5,10,15,20-tetrakis(phenyl)porphyrin shifts to shorter wavelengths in more polar solvents [23]. Thus, it was proposed that the dielectric properties of the environment, especially the partial negative charges on solvent molecules, change the mutual distance of central hydrogen ions. In highly polar solvents, this effect leads to displacement of central protons closer to each other and out of the macrocycle plane, producing a shift in the porphyrin spectrum [23,24].

The steady-state fluorescence emission spectra of these porphyrins were analyzed in DMF (Fig. 2). The two bands around 650 and 725 nm are characteristic for similar *meso*-substituted porphyrin. These bands have been assigned to $Q_x(0–0)$ and $Q_x(0–1)$ transitions [20]. This is a typical behavior for porphyrins with D_{2h} symmetry, like the free bases, and indicates that the porphyrin vibronic structure remains practically unchanged upon excitation [19]. Both TAPP and $TAPP^{4+}$ showed fluorescence spectra in water (Fig. 2, inset). In aqueous medium, the maximum of the emission of $TAPP^{4+}$ is shifted bathochromically with respect to that of TAPP by ~4 nm. The fluorescence quantum yields (Φ_F) of these porphyrins were calculated in DMF, giving values of 0.15 ± 0.01 and 0.13 ± 0.01 for TAPP and $TAPP^{4+}$, respectively. These Φ_F are very similar to that reported previously for $TMAP^{4+}$ in the same solvent (Φ_F = 0.12)

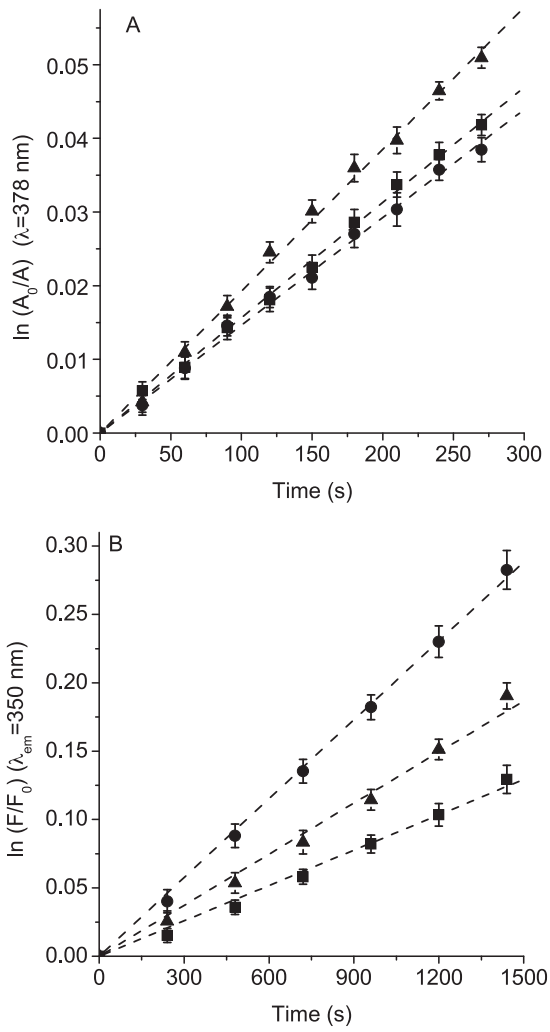

Fig. 3. First-order plots for the photooxidation of (A) DMA (35 μM, λ_{irr} = 420 nm) and (B) Trp (20 μM, λ_{irr} = 350–800 nm), photosensitized by in DMF. Values represent mean ± standard deviation of three separate experiments.

and they are suitable values for quantification and detection of the porphyrin in biological media [10].

3.2. Photosensitized decomposition of substrates in organic solvents

Photooxidation of DMA sensitized by these porphyrins was studied in DMF under aerobic condition (Fig. 3A). The values of the observed rate constant (k_{obs}^{DMA}) were calculated from first-order kinetic plots of the DMA absorption at 378 nm with time (Table 1). As can be observed, TAPP and $TAPP^{4+}$ photosensitized the decomposition of DMA with similar rates. DMA photooxidation was used as a method to evaluate the ability of the sensitizers to produce

Table 1
Kinetic parameters for the photooxidation reaction of DMA (k_{obs}^{DMA}) and Trp (k_{obs}^{Trp}), and singlet molecular oxygen quantum yield (Φ_{Δ}^{DMF}) in DMF.

Porphyrin	k_{obs}^{DMA} (s^{-1})[a]	Φ_{Δ}^{DMF}	k_{obs}^{Trp} (s^{-1})[c]
TAPP	$(1.56 \pm 0.05) \times 10^{-4}$	0.53 ± 0.02	$(9.8 \pm 0.3) \times 10^{-5}$
$TAPP^{4+}$	$(1.46 \pm 0.05) \times 10^{-4}$	0.49 ± 0.02	$(2.7 \pm 0.3) \times 10^{-4}$
$TMAP^{4+}$	$(1.92 \pm 0.06) \times 10^{-4}$	0.65[b]	$(1.4 \pm 0.3) \times 10^{-4}$

[a] λ_{irr} = 420 nm.
[b] From Ref. [5].
[c] λ_{irr} = 350–800 nm.

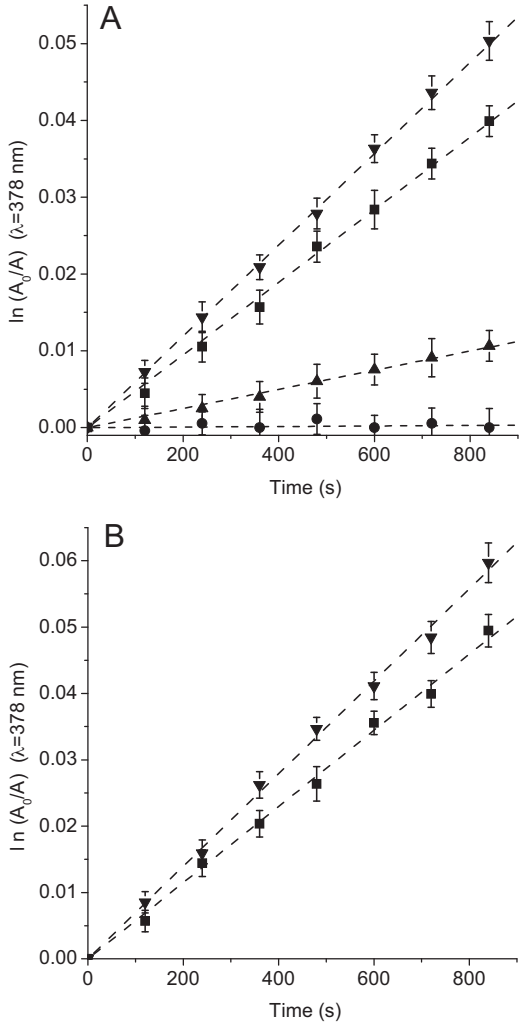

Fig. 4. First-order plots for the photooxidation of DMA (35 μM, λ_{irr} = 420 nm) photosensitized by TAPP (■), $TAPP^{4+}$ (•), $TMAP^{4+}$ (▲) and TPP (▼) in (A) THF and (B) toluene. Values represent mean ± standard deviation of three separate experiments.

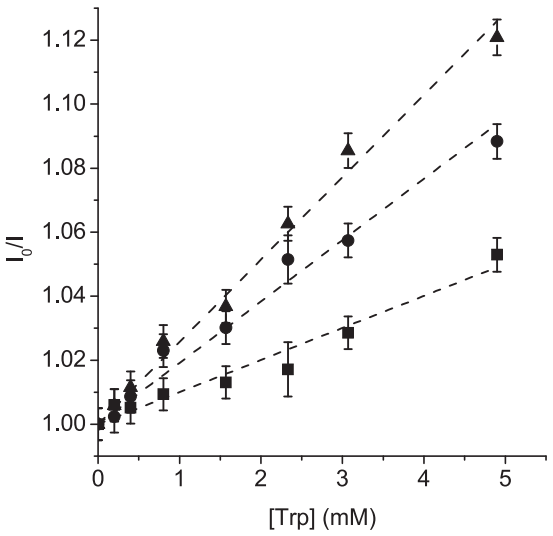

Fig. 5. Fluorescence intensity of TAPP (■), $TAPP^{4+}$ (•) and $TMAP^{4+}$ (▲) (λ_{exc} = 515 nm) in the presence of different Trp concentrations in DMF. Dashed line: curve regression fit by Eq. (1). Values represent mean ± standard deviation of three separate experiments.

$O_2(^1\Delta_g)$ in solution because it quenches $O_2(^1\Delta_g)$ exclusively by chemical reaction [25]. Thus, the quantum yield of $O_2(^1\Delta_g)$ production (Φ_Δ) were calculated by comparing the slope for the porphyrin with that for the reference ($TMAP^{4+}$) from the plots shown in Fig. 3A. Comparable values of Φ_Δ were obtained for TAPP and $TAPP^{4+}$ in DMF (Table 1), which are quite reasonable values for free base porphyrins dissolved as monomers [26]. A similar Φ_Δ value (0.51) was previously reported for $TAPP^{4+}$ in DMF using 5,10,15,20-tetraphenylporphyrin (TPP) as a reference [5].

Also, photodecomposition of DMA was studied in THF and toluene (Fig. 4). In both solvents, TPP was used as a reference because this porphyrin is dissolved in monomeric form [27,28]. The results of k_{obs}^{DMA} are summarized in Table 2. As can be seen, the photodynamic activity of uncharged porphyrins, TAPP and TPP, remained high in both solvents. However, the ability to produce $O_2(^1\Delta_g)$ decreased in presence of cationic porphyrins. This effect is mainly remarkable for $TAPP^{4+}$, which was not dissolved as monomer in THF. Moreover, the production of $O_2(^1\Delta_g)$ was negligible for $TAPP^{4+}$ and $TMAP^{4+}$ in toluene, according with their insolubilities in this apolar solvent.

On the other hand, photosensitized decomposition of Trp was investigated in DMF. This amino acid can be a potential target of the photodynamic activity induced by porphyrins in cells. Moreover, Trp can be efficiently photooxidized by both type I and type II reaction mechanisms [27]. As shown in Fig. 3B, the photooxidation followed first-order kinetics with respect to Trp concentration. From the plots in Fig. 3B, the values of the k_{obs}^{Trp} were calculated for Trp decomposition. The results shown in Table 1 indicate a higher value of k_{obs} for the reaction photosensitized by cationic porphyrins. These results are not in agreement with the $O_2(^1\Delta_g)$ production observed using photooxidation of DMA. Possibly, interactions between these porphyrins and Trp can be favoring an electron transfer process in the decomposition of Trp [29]. Thus, the interaction of the porphyrin singlet excited state with Trp was studied by steady-state fluorescence. Fig. 5 shows the Stern-Volmer plots of porphyrins at different Trp concentration in DMF. From Eq. (1), K_{SV} values of 10.0 ± 0.5, 19.2 ± 0.7, 25.7 ± 0.7 M^{-1} were obtained for TAPP, $TAPP^{4+}$ and $TMAP^{4+}$, respectively. Taking into account a τ_0 = 11.6 ns for $TMAP^{4+}$ in DMF [13], k_q was calculated given a value of 2.2×10^9 s^{-1}. Thus, the quenching rate constant by Trp of the singlet state of $TMAP^{4+}$ is near the diffusion limit in DMF. Considering a $\tau_0 \sim 10$ ns for free-base porphyrin in DMF [17], the same order of magnitude of k_q is expected for TAPP and $TAPP^{4+}$.

Table 2
Kinetic parameters for the photooxidation reaction of DMA (k_{obs}^{DMA}) and singlet molecular oxygen quantum yield (Φ_Δ^{DMF}) in THF and toluene.

Porphyrin	k_{obs}^{DMA} (s^{-1})[a]	Φ_Δ^{THF}	k_{obs}^{DMA} (s^{-1})[c]	$\Phi_\Delta^{toluene}$
TAPP	$(4.73 \pm 0.06) \times 10^{-5}$	0.49 ± 0.02	$(5.74 \pm 0.07) \times 10^{-5}$	0.51 ± 0.02
$TAPP^{4+}$	$(3.69 \pm 0.07) \times 10^{-7}$	$(4.0 \pm 0.5) \times 10^{-3}$	–	–
$TMAP^{4+}$	$(1.24 \pm 0.04) \times 10^{-5}$	0.13 ± 0.01	–	–
TPP	$(5.94 \pm 0.07) \times 10^{-5}$	0.62[b]	$(6.97 \pm 0.08) \times 10^{-5}$	0.62[b]

[a] THF, λ_{irr} = 420 nm.
[b] From Ref. [16].
[c] Toluene, λ_{irr} = 420 nm.

Table 3
Kinetic parameters for the photooxidation reaction of ABMM (k_{obs}^{ABMM}) and Trp (k_{obs}^{Trp}), and singlet molecular oxygen quantum yield (Φ_{Δ}^{water}) in water.

Porphyrin	k_{obs}^{ABMM} (s^{-1})[a]	k_{obs}^{Trp} (s^{-1})[b]
TAPP	$(4.4 \pm 0.2) \times 10^{-5}$	$(1.5 \pm 0.3) \times 10^{-5}$
$TAPP^{4+}$	$(5.4 \pm 0.2) \times 10^{-5}$	$(4.0 \pm 0.3) \times 10^{-5}$
$TMAP^{4+}$	$(1.8 \pm 0.1) \times 10^{-5}$	$(2.3 \pm 0.3) \times 10^{-4}$

[a] λ_{irr} = 423 nm.
[b] λ_{irr} = 350–800 nm.

However, the deactivation of porphyrins by an energy transfer mechanism can be ruled out on energetics grounds (E_s = 1.89, 1.90 and 1.91 eV for TAPP, $TAPP^{4+}$ and $TMAP^{4+}$, respectively; E_s = 3.51 eV for Trp [11]) and due to the lack of appropriate spectral properties [30]. Therefore photoinduced electron transfer must be considered. It was possible to estimate the driving force of electron transfer from Rehm-Weller expressions as previously described in water [30]. Taking into account a value of 0.43 V for the first reduction potential of $TMAP^{4+}$ [31] and of 1.02 V for the oxidation potential of Trp [32] in water *vs.* the normal hydrogen electrode, the detected quenching should be attributed to electron transfer from Trp to the porphyrin.

3.3. Photodynamic activity in water

Anthracene derivatives with hydrophilic substituents can serve as $O_2(^1\Delta_g)$ traps in aqueous solution [33]. The addition of carboxylic groups to DMA is an interesting option. Thus, ABMA was first used for the detection of $O_2(^1\Delta_g)$ formation in water. However, ABMA contains four carboxylic acid groups that at a concentration of 35 μM was sufficient to partially protonate the tetrapyrrolic macrocycle. Under this condition, the absorption spectra of the porphyrins showed bands at 450 nm and 670 nm, which are typical of protonated *meso*-substituted porphyrin [34]. Therefore, the salt derivative ABMM was synthetized and used as a molecular probe for the detection of $O_2(^1\Delta_g)$ in water. The chemical trapping of $O_2(^1\Delta_g)$ ABMM leads to the formation of 9,10-endoperoxide product ABMM-O_2. The conversion allows follow the loss of absorption at 378 nm for its correlation to the proportional quantity of $O_2(^1\Delta_g)$ produced due to the high kinetic rate constant of the trapping reaction in aqueous media [35]. In the presence of porphyrin, a fast loss of ABMM absorption at 378 nm was observed in water (Fig. 6A). Even though the lifetime of $O_2(^1\Delta_g)$ in water is known to be as short as 4 μs, which is 6-fold less than in DMF [36], the use of ABMM as the $O_2(^1\Delta_g)$ acceptor was proven to be effective for the determination of quantum efficiency in water. This is due to its extremely high water-solubility with four carboxylate salts per anthracene molecule that enables intervening in the rapid trapping reaction [9]. As shown in Table 3, similar values of reaction rates were found for ABMM decomposition photosensitized by TAPP and $TAPP^{4+}$. In contrast, a lower value of k_{obs}^{ABMM} was obtained using $TMAP^{4+}$. A disadvantage of ABMM anionic trap is the interaction with cationic photosensitizers mainly when the cationic groups are directly linked to the tetrapyrrolic macrocycle, such as $TMAP^{4+}$. The interaction of ABMM with this photosensitizer can significantly interfere in the $O_2(^1\Delta_g)$ generation [33]. Therefore, we compared the results in Table 3 with that using $TPPS^{4-}$ as an anionic photosensitizer. Furthermore, it is known that the $TPPS^{4-}$ presents an efficient photodynamic activity in water (Φ_{Δ} = 0.74 [37]) similar to that of $TMAP^{4+}$ (Φ_{Δ} = 0.77 [38]). The photooxidation of ABMM induced by $TPPS^{4-}$ gave a value of $k_{obs}^{ABMM} = (1.0 \pm 0.1) \times 10^{-4} s^{-1}$, which was faster than those found using cationic porphyrins (Table 3). This anionic porphyrin repels ABMM avoiding interactions with the tetrapyrrolic macrocycle and keeping its $O_2(^1\Delta_g)$ production. As can be observed in Table 3, the photodynamic activity of TAPP and $TAPP^{4+}$ were less affected than $TMAP^{4+}$ by the presence ABMM. In these porphyrins, the cationic centers are isolated from the tetrapyrrolic macrocycle by a propoxy bridge. Thus, the charges have minimal influence on the electronic density of the porphyrin macrocycle. Furthermore, photooxidation of Trp sensitized by these porphyrins was studied in water (Fig. 6B). The results are shown in Table 3. A higher value of k_{obs}^{Trp} was found using $TMAP^{4+}$ as photosensitizer. This value is even higher than that found in DMF (Table 1). In contrast, values of k_{obs}^{Trp} photosensitized by TAPP and $TAPP^{4+}$ decreased ~7 times with respect to those in DMF. In water, these porphyrins are not completely dissolved as monomers, as shown by a small broadening of the Soret band (Fig. 1), and this partial aggregation precluded the photodynamic activity.

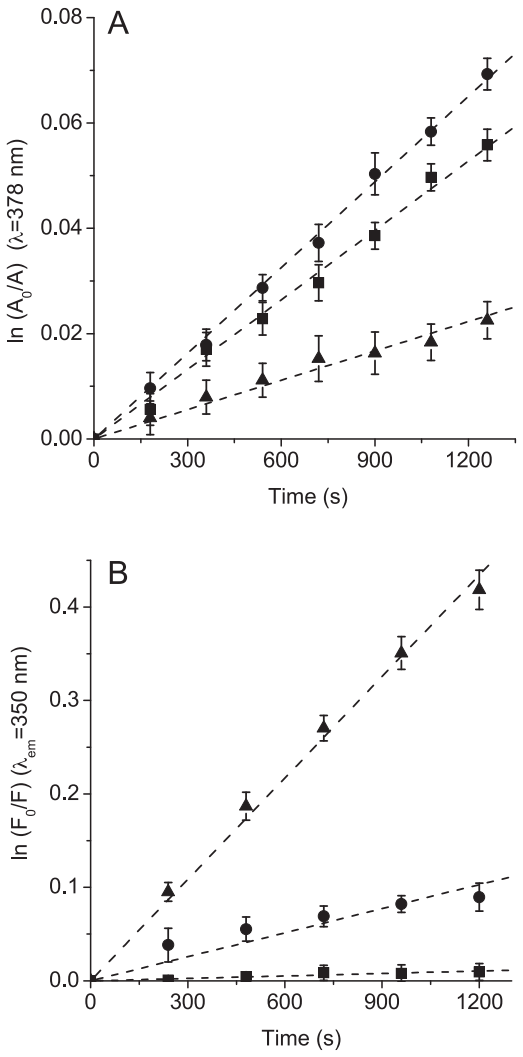

Fig. 6. First-order plots for the photooxidation of (A) ABMM (35 μM, λ_{irr} = 423 nm) and (B) Trp (20 μM, λ_{irr} = 350–800 nm), photosensitized by TAPP (■), $TAPP^{4+}$ (●) and $TMAP^{4+}$ (▲) in water. Values represent mean ± standard deviation of three separate experiments.

3.4. Interaction with β-CD and sensitized oxidation of substrates

The presence of cyclodextrin forming supramolecular assemblies with porphyrin can be used to provide a microscopically apolar environment around the center of a porphyrin ring and these inclusion complexes can be used to deliver the photosensitizer in different media [39]. Therefore, the effects of the addition of β-CD

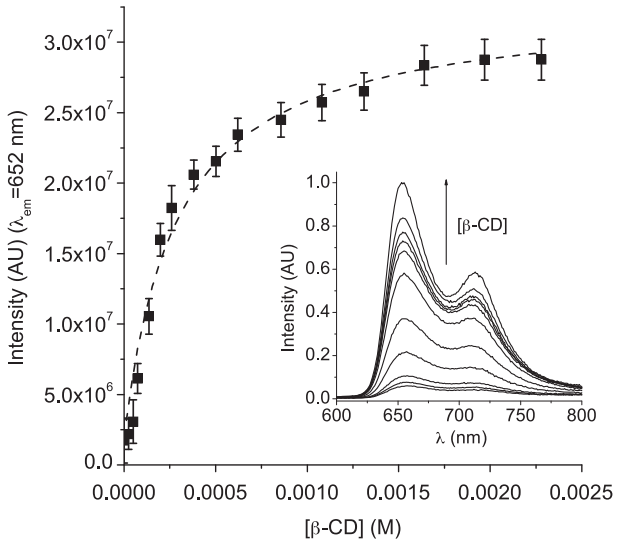

Fig. 7. Fluorescence intensity of $TAPP^{4+}$ (λ_{exc} = 422 nm, λ_{em} = 465 nm) in the presence of different β-CD concentrations. Dashed line: curve regression fit by Eq. (2), n = 1. Inset: emission spectra of $TAPP^{4+}$ at different β-CD concentrations (0.025–2.8 mM). Values represent mean ± standard deviation of three separate experiments.

on the fluorescence properties of porphyrins were investigated in water. Addition of β-CD to an aqueous solution of $TAPP^{4+}$ produces an increase in the overall emission intensity of porphyrin fluorescence compared to that observed in bulk water (Fig. 7, inset). These changes suggest an interaction of β-CD with $TAPP^{4+}$. As shown, the increase of the β-CD concentrations produced an important enhancement of the complex fluorescence intensity. At higher β-CD concentrations, only small intensity variation was observed. The experimental data were fitted by Eq. (2), which provides the basic for the determination of stoichiometric ratio and binding constant ($K_{\beta\text{-CD}}$). The result shows in Fig. 7 indicates that the curve fit by Eq. (2) with n = 1 was the best one to represent the experimental data. This result indicates a 1:1 complex ratio of β-CD only to $TAPP^{4+}$ in aqueous solution. The value of $K_{\beta\text{-CD}}$ calculated was 3500 ± 500 M^{-1}. The interaction of $TAPP^{4+}$ with β-CD can be enhanced by the aliphatic spacer between the cationic groups and the tetrapyrrole macrocycle [39]. In contrast, no significant changes were observed for TAPP and $TMAP^{4+}$, possibly because the interaction with β-CD is smaller and it can not be detected by this methodology. Also, it was previously found that $TMAP^{4+}$, whose cationic peripheries are attached directly to the porphyrin ring, formed very unstable complexes with any cyclodextrin [39].

The $O_2(^1\Delta_g)$ trap ABMM was used to evaluate the photodynamic activity by these porphyrins in aqueous media containing β-CD (Fig. 8A). The results in Table 4 show that the value of k_{obs}^{ABMM} sensitized by $TMAP^{4+}$ was similar in presence of β-CD with that in pure water. The complex of $TMAP^{4+}$ with β-CD is very weak and, as previously found in water, this cationic porphyrin interact strongly with ABMM. Therefore, the addition of β-CD does not affect the value of k_{obs}^{ABMM} found in water. Photodecomposition rate of ABMM induced by TAPP and $TAPP^{4+}$ were lower in presence of β-CD than in water (Table 3). It was shown by spectroscopic studies that β-CD forms inclusion complexes with anthracene derivatives [40]. In water, the photodynamic activity of TAPP and $TAPP^{4+}$ were less affected by ABMM than for $TMAP^{4+}$. Therefore, β-CD could be preventing ABMM decomposition by $O_2(^1\Delta_g)$ in presence of TAPP and $TAPP^{4+}$.

Photooxidation of Trp was investigated in β-CD aqueous solution (Fig. 8B). A can be observed in Table 4, similar values for k_{obs}^{Trp} were found in solution of β-CD and in water. Thus, the presence of β-CD is not affecting the photodynamic activity of these porphyrins to produce Trp photooxidation. These results were expected for TAPP and $TMAP^{4+}$ since these porphyrins not interact with β-CD and apparently the complex with $TAPP^{4+}$ does not affect its photodynamic properties to photooxidize Trp.

Table 4
Kinetic parameters for the photooxidation reaction of ABMM (k_{obs}^{ABMM}) and Trp (k_{obs}^{Trp}) in β-CD (0.0025 M) aqueous solution.

Porphyrin	k_{obs}^{ABMM} (s^{-1})[a]	k_{obs}^{Trp} (s^{-1})[b]
TAPP	$(1.7 \pm 0.3) \times 10^{-5}$	$(1.8 \pm 0.3) \times 10^{-5}$
$TAPP^{4+}$	$(2.6 \pm 0.3) \times 10^{-5}$	$(4.1 \pm 0.3) \times 10^{-5}$
$TMAP^{4+}$	$(2.1 \pm 0.3) \times 10^{-5}$	$(2.5 \pm 0.3) \times 10^{-4}$

[a] λ_{irr} = 423 nm.
[b] λ_{irr} = 350–800 nm.

3.5. Solubilization and photodynamic activity in AOT reverse micelles

The solubilization and interaction of these cationic porphyrins were spectroscopically analyzed in n-heptane/AOT (0.1 M)/water (W_0 = 10) reverse micelles. This microheterogeneous medias have been frequently used as an interesting model to mimic the water pockets often found in various bioaggregates such as proteins,

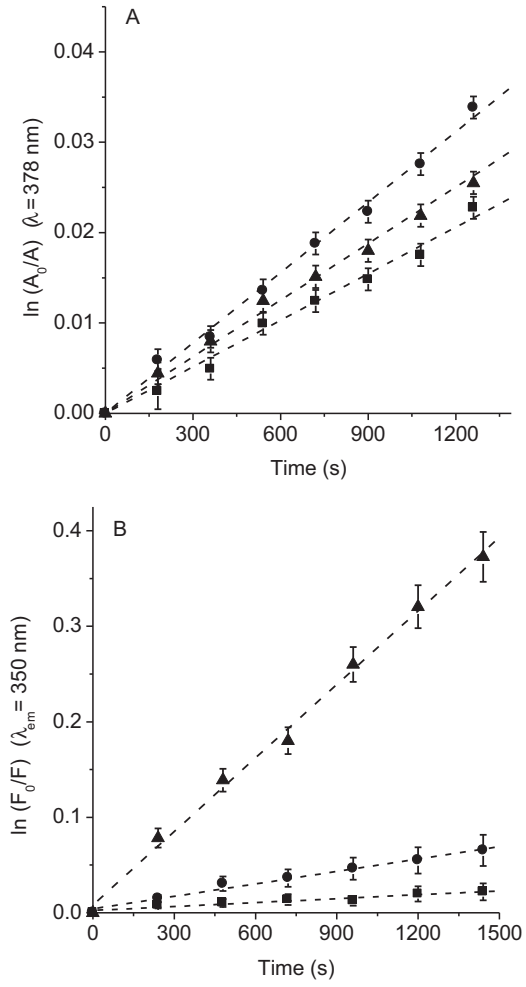

Fig. 8. First-order plots for the photooxidation of (A) ABMM (35 μM, λ_{irr} = 423 nm) and (B) Trp (20 μM, λ_{irr} = 350–800 nm), photosensitized by TAPP (■), $TAPP^{4+}$ (●) and $TMAP^{4+}$ (▲) in β-CD (0.025 M) aqueous solution. Values represent mean ± standard deviation of three separate experiments.

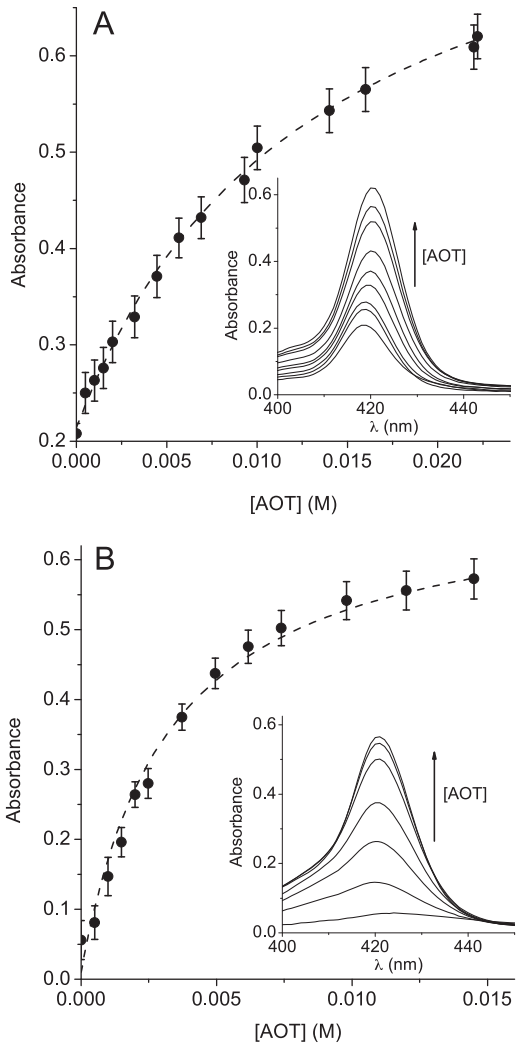

Fig. 9. Variation of absorption as a function of [AOT] in *n*-heptane/AOT/water ($W_0 = 10$) reverse micelles ($\lambda_{max} = 422$ nm) of (A) TAPP and (B) TAPP^{4+}. Dashed line: no linear regression fit by Eq. (3). Inset: absorption spectra of TAPP^{4+} at different AOT concentrations (0.2–2.0 mM). Values represent mean ± standard deviation of three separate experiments.

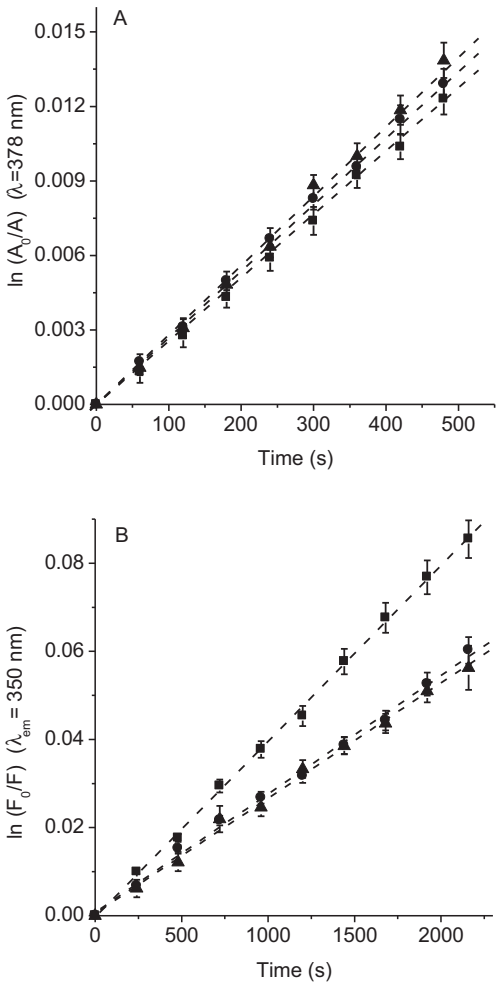

Fig. 10. First-order plots for the photooxidation of (A) DMA (35 μM, $\lambda_{irr} = 420$ nm) and (B) Trp (20 μM, $\lambda_{irr} = 350$–800 nm), photosensitized by TAPP (■), TAPP^{4+} (•) and TMAP^{4+} (▲) in *n*-heptane/AOT (0.1 M)/water ($W_0 = 10$) reverse micelles. Values represent mean ± standard deviation of three separate experiments.

enzymes and membranes [41]. In micellar systems, a solute can be located in a variety of microenvironments, namely the organic surrounded solvent, the water pool or at the micellar interface [14]. When the absorption spectra of porphyrins were studied at various AOT concentrations, an increase in the intensity of the *Soret* band was observed for TAPP and TAPP^{4+} as the surfactant concentration increased. Representative results for TAPP and TAPP^{4+} are shown in Fig. 9 inset. This effect was attributed to the interaction between the porphyrin and the AOT micelles. Plotting the Soret band absorption *vs.* AOT concentration, the value of the distribution constant (K_{AOT}) was calculated by fitting Eq. (3) (Fig. 9). Values of $K_{AOT} = 77 \pm 8\ M^{-1}$ for the TAPP and $K_{AOT} = 307 \pm 25\ M^{-1}$ for the TAPP^{4+} indicate that these photosensitizers are associated with the micellar interface. The presence of intrinsic positive charges in the macrocycle of TAPP^{4+} produces a higher interaction with AOT reverse micelles in comparison with its homologue containing amino groups. Also, spectroscopic changes for TMAP^{4+} showed that interact significantly with the micellar interface [13].

Photooxidation of DMA sensitized by these porphyrins was performed in *n*-heptane/AOT (0.1 M)/water ($W_0 = 10$) under aerobic conditions. Because DMA is a non-polar compound, it is assumed that this substrate is mainly solubilized in the organic pseudophase (*n*-heptane) of the micellar system [42]. In this biomimetic microenvironment, the substrate reacts with the $O_2(^1\Delta_g)$ photosensitized by porphyrin. From the plots in Fig. 10A, the values of the k_{obs}^{DMA} were calculated for DMA reaction in micellar system. As can be observed in Table 5, the decomposition of DMA sensitized by these porphyrins follow the tendency found in DMF. Thus, TAPP and TAPP^{4+} were efficient photosensitizers to generate $O_2(^1\Delta_g)$ in this microheterogeneous medium. However, the reaction rates of DMA in the AOT micellar system (Table 5) were ~6 times slower than those found in DMF (Table 1) by a factor of 6. Similar behavior was previously observed in AOT reverse micelles using porphyrins as photosensitizers [43]. In the AOT micellar system, $O_2(^1\Delta_g)$ is partitioned between the internal and external pseudophases with

Table 5
Kinetic parameters for the photooxidation reaction of DMA (k_{obs}^{DMA}) and Trp (k_{obs}^{Trp}) in *n*-heptane/AOT (0.1 M)/H_2O ($W_0 = 10$).

Porphyrin	k_{obs}^{DMA} (s^{-1})[a]	k_{obs}^{Trp} (s^{-1})[b]
TAPP	$(2.2 \pm 0.1) \times 10^{-5}$	$(3.6 \pm 0.3) \times 10^{-5}$
TAPP^{4+}	$(2.4 \pm 0.1) \times 10^{-5}$	$(2.5 \pm 0.3) \times 10^{-5}$
TMAP^{4+}	$(2.9 \pm 0.1) \times 10^{-5}$	$(2.3 \pm 0.3) \times 10^{-5}$

[a] $\lambda_{irr} = 420$ nm.
[b] $\lambda_{irr} = 350$–800 nm.

a partition constant of 0.11 [42]. Therefore, the photooxidation rate of DMA was diminished in the organic pseudophase.

When Trp photooxidation was studied in AOT reverse micelles, the disappearance of the amino acid following the behavior showed in Fig. 10B. A value of k_{obs}^{Trp} higher was obtained for the reaction sensitized by TAPP with respect to cationic porphyrins (Table 5). The value k_{obs}^{Trp} induced by $TMAP^{4+}$ diminished in AOT micelles with respect to that in water. This effect was also observed using a tetracationic zinc(II)tetramethyltetrapyridino[2,3-*b*:2′,3′-*g*:2″,3″-*l*:2‴,3‴-*q*]porphyrazinium as photosensitizer [44]. In AOT micellar system, porphyrins can be located in different microenvironments depending on their structure. Since $TMAP^{4+}$ has opposite charges of the surfactant forming the micelle, it is effectively bound to the AOT anionic micelles head groups [13]. Likewise in the case of $TAPP^{4+}$, intrinsic cationic charges could promote electrostatic attraction of this cationic porphyrin with the AOT head groups, avoiding direct interaction with the amino acid. However, the non-charged photosensitizer TAPP can be located in a different microenvironment of the micellar interface, which allowed to TAPP remains a similar photodynamic activity to decompose Trp than that obtained in DMF.

4. Conclusions

This study provides information on the photodynamic activity of TAPP and $TAPP^{4+}$ in different media. The $O_2(^1\Delta_g)$ production is efficiently photosensitized by both porphyrins with $\Phi_\Delta \sim 0.5$ in DMF. However, the values of Φ_Δ can significantly change in a different medium, diminishing mainly when the photosensitizer is partially aggregated. Decomposition of ABMM, as $O_2(^1\Delta_g)$ molecule trap, diminished in water due to the interaction with TAPP and $TAPP^{4+}$. This decrease was not as pronounced as that found for $TMAP^{4+}$, due to the presence of an aliphatic spacer between the cationic groups and the porphyrin ring in TAPP and $TAPP^{4+}$. In β-CD solution, photooxidation of ABMM by TAPP and $TAPP^{4+}$ diminished with respect to water, probably due to an interaction between ABMM and β-CD. In AOT system, all of these porphyrins strongly interact with the reverse micelles. In this microheterogenic medium, TAPP and $TAPP^{4+}$ have similar photodynamic effect as found for $TMAP^{4+}$. Photooxidation of Trp sensitized by $TAPP^{4+}$ was higher than TAPP in homogenic media and in β-CD solution. However, the behavior was inverted in AOT reverse micelles. In this media, Trp is dissolved in the water pool avoiding interaction with cationic porphyrins, which are bound to the AOT anionic micelles head groups. These results indicate that $O_2(^1\Delta_g)$ production is highly dependent on the medium where the sensitizer is localized and decreases when the sensitizer is aggregated. Thus, photodynamic properties of the porphyrins established in solution can be significantly modified in the biological microenvironment where the sensitizer is localized. However, it is expected that of all media studied in this work, AOT reverse micelles are best represents a biological membrane and in this system is where TAPP showed a higher photodynamic activity in comparison with the cationic porphyrins. Therefore, TAPP can be a good candidate, even without intrinsic cationic charges, for the photodynamic inactivation of microorganisms.

Acknowledgements

Authors are grateful to Consejo Nacional de Investigaciones Científicas y Técnicas (CONICET) of Argentina, SECYT Universidad Nacional de Río Cuarto, MINCyT Córdoba and Agencia Nacional de Promoción Científica y Tecnológica (FONCYT) for financial support. M.E.M. and E.N.D. are Scientific Members of CONICET. S.J.M. thanks CONICET for a doctoral fellowship.

References

[1] T. Dai, Y.Y. Huang, M.R. Hamblin, Photodynamic therapy for localized infections-state of the art, Photodiagnosis and Photodynamic Therapy 6 (2009) 170–188.
[2] E.N. Durantini, Photodynamic inactivation of bacteria, Current Bioactive Compounds 2 (2006) 127–142.
[3] T.G. Denis St., T. Dai, L. Izikson, C. Astrakas, R.R. Anderson, M.R. Hamblin, G.P. Tegos, All you need is light. Antimicrobial photoinactivation as an evolving and emerging discovery strategy against infectious disease, Virulence 2 (2011) 509–520.
[4] J.P.C. Tomé, M.G.P.M.S. Neves, A.C. Tomé, J.A.S. Cavaleiro, M. Soncin, M. Magaraggia, S. Ferro, G. Jori, Synthesis and antibacterial activity of new poly-S-lysine-porphyrin conjugates, Journal of Medicinal Chemistry 47 (2004) 6649–6652.
[5] D.A. Caminos, M.B. Spesia, E.N. Durantini, Photodynamic inactivation of *Escherichia coli* by novel *meso*-substituted porphyrins by 4-(3-*N*,*N*,*N*-trimethylammoniumpropoxy) phenyl and 4-(trifluoromethyl)phenyl groups, Photochemical & Photobiological Sciences 5 (2006) 56–65.
[6] D.A. Caminos, E.N. Durantini, Synthesis of asymmetrically meso-substituted porphyrins bearing amino groups as potential cationic photodynamic agents, Journal of Porphyrins and Phthalocyanines 9 (2005) 334–342.
[7] D.A. Caminos, M.B. Spesia, P. Pons, E.N. Durantini, Mechanisms of *Escherichia coli* photodynamic inactivation by an amphiphilic tricationic porphyrin and 5,10,15, 20-tetra(4-N,N,N-trimethylammoniumphenyl)porphyrin, Photochemical & Photobiological Sciences 7 (2008) 1071–1078.
[8] M.P. Cormick, E.D. Quiroga, S.G. Bertolotti, M.G. Alvarez, E.N. Durantini, Mechanistic insight of the photodynamic effect induced by tri- and tetra-cationic porphyrins on *Candida albicans* cells, Photochemical & Photobiological Sciences 10 (2011) 1556–1561.
[9] M. Wang, S. Maragani, L. Huang, S. Jeon, T. Canteenwala, M.R. Hamblin, L.Y. Chiang, Synthesis of decacationic [60]fullerene decaiodides giving photoinduced production of superoxide radicals and effective PDT-mediation on antimicrobial photoinactivation, European Journal of Medicinal Chemistry 63 (2013) 170–184.
[10] M.P. Cormick, M.G. Alvarez, M. Rovera, E.N. Durantini, Photodynamic inactivation of *Candida albicans* sensitized by tri- and tetra-cationic porphyrin derivatives, European Journal of Medicinal Chemistry 44 (2009) 1592–1599.
[11] M.E. Daraio, A. Völker, P.F. Aramendia, E. San Roman, tryptophan quenching of zinc-phthalocyanine and porphycene fluorescence in micellar CTAC, Photochemistry and Photobiology 67 (1998) 371–377.
[12] R. Yang, K. Wang, D. Xiao, X. Yang, Fluorometric study of the inclusion interaction of β-cyclodextrin derivatives with tetraphenylporphyrin and its analytical application, Spectrochimica Acta Part A 57 (2001) 1595–1602.
[13] M. Novaira, M.P. Cormick, E.N. Durantini, Spectroscopic and time-resolved fluorescence emission properties of a cationic and an anionic porphyrin in biomimetic media and *Candida albicans* cells, Journal of Photochemistry and Photobiology A: Chemistry 246 (2012) 67–74.
[14] J.J. Silber, A. Biasutti, E. Abuin, E. Lissi, Interactions of small molecules with reverse micelles, Advances in Colloid and Interface Science 82 (1999) 189–252.
[15] D.A. Caminos, E.N. Durantini, A simple experiment to show photodynamic inactivation of bacteria on surfaces, Biochemistry and Molecular Biology Education 35 (2007) 64–69.
[16] R. Schmidt, E. Afshari, Effect of solvents on the phosphorescence rate constant of singlet molecular oxygen ($^1\Delta_g$), Journal of Physical Chemistry 94 (1990) 4377–4378.
[17] M.E. Milanesio, M.G. Alvarez, S.G. Bertolotti, E.N. Durantini, Photophysical characterization and photodynamic activity of metallo 5-(4-(trimethylammonium)phenyl)-10, 15,20-tris(2,4,6-trimethoxyphenyl) porphyrin in homogeneous and biomimetic media, Photochemical & Photobiological Sciences 7 (2008) 963–972.
[18] T. Hashimoto, Y.-K. Choe, H. Nakano, K. Hirao, Theoretical study of the Q and B bands of free-base, magnesium, and zinc porphyrins, and their derivatives, Journal of Physical Chemistry A 103 (1999) 1894–1904.
[19] R.V. Maximiano, E. Piovesan, S.C. Zílio, A.E.H. Machado, R. de Paula, J.A.S. Cavaleiro, I.E. Borissevitch, A.S. Ito, P.J. Gonçalves, N.M. Barbosa Neto, Excited-state absorption investigation of a cationic porphyrin derivative, Journal of Photochemistry and Photobiology A: Chemistry 214 (2010) 115–120.
[20] J.S. Baskin, H.-Z. Yu, A.H. Zewail, Ultrafast dynamics of porphyrins in the condensed phase: I. Free base tetraphenylporphyrin, Journal of Physical Chemistry A 106 (2002) 9837–9844.
[21] M. Makarska, St. Radzki, J. Legendziewicz, Spectroscopic characterization of the water-soluble cationic porphyrins and their complexes with Cu(II) in various solvents, Journal of Alloys and Compounds 341 (2002) 233–238.
[22] M. Makarska-Bialokoz, G. Pratviel, St. Radzki, The influence of solvent polarity on spectroscopic properties of 5-[4-(5-carboxy-1-butoxy)-phenyl]-10, 15,20-tris(4-N-methylpyridiniumyl) porphyrin and its complexes with Fe(III) and Mn(III) ions, Journal of Molecular Structure 875 (2008) 468–477.
[23] I. Renge, Solvent dependence of the visible absorption maxima of *meso*-tetraphenylporphine, Chemical Physics Letters 185 (1991) 231–236.
[24] I. Renge, Solvent effects on the visible absorption maxima of tetrapyrrolic pigments, Journal of Physical Chemistry 97 (1993) 6582–6589.
[25] A. Gomes, E. Fernandes, J.L.F.C. Lima, Fluorescence probes used for detection of reactive oxygen species, Journal of Biochemical and Biophysical Methods 65 (2005) 45–80.

[26] R.W. Redmond, J.N. Gamlin, A compilation of singlet yields from biologically relevant molecules, Photochemistry and Photobiology 70 (1999) 391–475.
[27] M.E. Milanesio, M.G. Alvarez, E.I. Yslas, C.D. Borsarelli, J.J. Silber, V. Rivarola, E.N. Durantini, Photodynamic studies of metallo 5, 10,15,20-tetrakis(4-methoxyphenyl)porphyrin: photochemical characterization and biological consequences in a human carcinoma cell line, Photochemistry and Photobiology 74 (2001) 14–21.
[28] M.E. Milanesio, M.G. Alvarez, V. Rivarola, J.J. Silber, E.N. Durantini, Porphyrin-fullerene C_{60} dyads with high ability to form photoinduced charge-separated state as novel sensitizers for photodynamic therapy, Photochemistry and Photobiology 81 (2005) 891–897.
[29] J.M. Wessels, C.S. Foote, W.E. Ford, M.A.J. Rodgers, Photooxidation of tryptophan: $O_2(^1\Delta_g)$ versus electron-transfer pathway, Photochemistry and Photobiology 65 (1997) 96–102.
[30] V.S. Chirvony, V.A. Galievsky, N.N. Kruk, B.M. Dzhagarov, P.-Y. Turpin, Photophysics of cationic 5,10, 15,20-tetrakis-(4-N-methylpyridyl)porphyrin bound to DNA, $[poly(dA\text{-}dT)]_2$ and $[poly(dG\text{-}dC)]_2$: on a possible charge transfer process between guanine and porphyrin in its excited singlet state, Journal of Photochemistry and Photobiology B: Biology 40 (1997) 154–162.
[31] Q. Feng, N.-Q. Li, Y.-Y. Jiang, Electrochemical studies of porphyrin interacting with DNA and determination of DNA, Analytica Chimica Acta 344 (1997) 97–104.
[32] M.R. DeFelippis, C.P. Murthy, F. Broitman, D. Weinraub, M. Faraggi, M.H. Klapper, Electrochemical properties of tyrosine phenoxy and tryptophan indolyl radicals in peptides and amino acid analogues, Journal of Physical Chemistry 95 (1991) 3416–3419.
[33] G.R. Martinez, F. Garcia, L.H. Catalani, J. Cadet, M.C.B. Oliveira, G.E. Ronsein, S. Miyamoto, M.H.G. Medeiros, P. Di Mascio, Synthesis of a hydrophilic and non-ionic anthracene derivative, the N,N′-di-(2,3-dihydroxypropyl)-9,10-anthracenedipropanamide as a chemical trap for singlet molecular oxygen detection in biological systems, Tetrahedron 62 (2006) 10762–10770.
[34] N.E. Mukundan, G. Pethö, D.W. Dixon, M.S. Kim, L.G. Marzilli, Interactions of an electron-rich tetracationic tentacle porphyrin with calf thymus DNA, Inorganic Chemistry 33 (1994) 4676–4687.
[35] K.I. Setsukinai, Y. Urano, K. Kakinuma, H.J. Majima, T. Nagano, Development of novel fluorescence probes that can reliably detect reactive oxygen species and distinguish specific species, Journal of Biological Chemistry 278 (2003) 3170–3175.
[36] F. Wilkinson, W.P. Helman, A.B. Ross, Rate constants for the decay and reactions of the lowest electronically excited singlet state of molecular oxygen in solution. An expanded and revised compilation, Journal of Physical and Chemical Reference Data 24 (1995) 663–1021.
[37] V. Gottfried, D. Peled, J.W. Winkelman, S. Kimel, Photosensitizers in organized media: singlet oxygen production and spectral properties, Photochemistry and Photobiology 48 (1988) 157–163.
[38] J.-B. Verlhac, A. Gaudemer, I. Kraljic, Water soluble porphyrins and metalloporphyrins as photosensitizers in aerated aqueous solutions. I. Detection and determination of quantum yield of formation of singlet oxygen, Nouveau Journal de Chimie 8 (1984) 401–406.
[39] K. Kano, R. Nishiyabu, T. Asada, Y. Kuroda, Static and dynamic behavior of 2:1 inclusion complexes of cyclodextrins and charged porphyrins in aqueous organic media, Journal of the American Chemical Society 124 (2002) 9937–9944.
[40] S.-I. Sato, Y. Yoshizumi, T. Kiba, A. Murayama, S. Abe, Spectral narrowing of UV–visible absorption and emission spectra of anthracene-derivatives in β-cyclodextrin nanocavity: effects of host/guest stoichiometry, Molecular Crystals and Liquid Crystals 568 (2012) 60–65.
[41] I. Scalise, E.N. Durantini, Photodynamic effect of metallo 5-(4-carboxyphenyl)-10, 15,20-tris(4-methylphenyl) porphyrins in biomimetic media, Journal of Photochemistry and Photobiology A: Chemistry 162 (2004) 105–113.
[42] C.D. Borsarelli, E.N. Durantini, N.A. García, Singlet molecular oxygen-mediated-photooxidation of nitrophenolic compounds in water-in-oil microemulsions, Journal of the Chemical Society, Perkin Transactions 2 (1996) 2009–2013.
[43] S.J. Mora, M.P. Cormick, M.E. Milanesio, E.N. Durantini, The photodynamic activity of a novel porphyrin derivative bearing a fluconazole structure in different media and against *Candida albicans*, Dyes and Pigments 87 (2010) 234–240.
[44] T.C. Tempesti, J.C. Stockert, E.N. Durantini, Photosensitization ability of a water soluble zinc(II)tetramethyltetrapyridinoporphyrazinium salt in aqueous solution and biomimetic reverse micelles medium, Journal of Physical Chemistry B 112 (2008) 15701–15707.